Scientific Contributions Oil & Gas, Vol. 49. No. 1, March: 375 - 397

SCIENTIFIC CONTRIBUTIONS OIL AND GAS

Testing Center for Oil and Gas
LEMIGAS

Journal Homepage:http://www.journal.lemigas.esdm.go.id
ISSN: 2089-3361, e-ISSN: 2541-0520

Designing A Compact 2×2 Dual-Band Mimo Microstrip Antenna for Wireless Monitoring Systems in Oil And Gas Facilities

Didik Aribowo[1,2], Zainuddin Nawawi[1], Bhakti Yudho Suprapto[1]

[1] Department of Electrical Engineering, Universitas Sriwijaya, Palembang,
Al-Ghazali Mosque Street, Bukit Lama, Ilir Barat I District, Palembang City, South Sumatra 30128, Indonesia.

[2] Department Of Electrical Engineering Vocational Education, Universitas Sultan Ageng Tirtayasa Serang Banten,
Jl. Raya Jakarta No.3, Sindangsari, Pabuaran District, Serang City, Banten 42163, Indonesia.

Corresponding Author : Didik Aribowo (d_aribowo@untirta.ac.id)

Manuscript received: January 1th, 2025; Revised: January 19th, 2026
Approved: January 20th, 2026; Available online: March 2th, 2026; Published: March 2th, 2026.

ABSTRACT - Oil and gas facilities present challenging wireless communication environments due to complex metallic structures and severe multipath propagation, which can degrade the reliability of Industrial Internet of Things (IIoT)–based monitoring systems. To address this issue, this study proposes a compact dual-band 2×2 MIMO microstrip antenna operating at 2.6 GHz and 3.8 GHz for wireless monitoring applications in oil and gas facilities. The antenna is fabricated on a low-cost FR-4 substrate and employs a hexagonal patch geometry, miniaturized using a beveled half-cut technique to shorten the effective current path while maintaining good impedance matching. Furthermore, a multi-bridge ground structure is introduced to reduce mutual coupling between MIMO elements. Antenna performance is evaluated through simulations using Computer Simulation Technology (CST) by analyzing S-parameters, VSWR, gain, and radiation patterns. Simulation results show that the proposed antenna achieves reflection coefficients below −10 dB at both operating bands, inter-element isolation of up to ≤ −20 dB, VSWR values below 1.5, and a peak gain of 1.41 dBi. These results indicate that the proposed compact dual-band MIMO antenna is a promising candidate for reliable wireless monitoring systems in oil and gas facilities.

Keywords: MIMO microstrip antenna, dual-band antenna, antenna miniaturization, wireless monitoring system for oil and gas facilities, industrial internet of things (IIoT)

How to cite this article:

Didik Aribowo, Zainuddin Nawawi, Bhakti Yudho Suprapto 2026, Designing A Compact 2×2 Dual-Band Mimo Microstrip Antenna for Wireless Monitoring Systems in Oil And Gas Facilities, Scientific Contributions Oil and Gas, 49 (1) pp. 375 - 397. DOI org/10.29017/scog.v49i1.1992

INTRODUCTION

The rapid development of telecommunication technology continues to reshape modern communication systems, driven by the evolution of cellular networks from 1G to 4G and the increasing demand for higher data rates, reliable connectivity, and flexible deployment. In industrial sectors, particularly oil and gas, wireless communication has become a critical enabler for real-time monitoring, automation, and operational safety. Applications such as SCADA systems, pipeline monitoring, equipment supervision, and industrial internet of things (IIoT) deployments rely heavily on stable wireless links in harsh environments with metallic structures, electromagnetic interference, and severe multipath propagation. In this context, antenna performance plays a central role, as it directly influences signal propagation, system efficiency, and overall communication reliability in oil and gas fields.

Within the 3GPP framework, long-term evolution (LTE) was introduced as an evolution of UMTS and HSPA, offering significantly higher throughput and improved spectral efficiency. Among LTE frequency allocations, mid-band spectrum has gained widespread adoption for its favorable balance of coverage and capacity.

Globally, LTE-E 2300 and LTE-D 2600 are widely deployed bands, with LTE-D 2600 remaining popular because of its broader contiguous allocation and strong device ecosystem support, although inter-system interference remains a challenge in dense deployment (Bharathi Kannan Maheswari, 2021). In Indonesia, the 2.3 GHz band has been refarmed to provide more contiguous spectrum, and economic assessments confirm its feasibility and cost-effectiveness for nationwide LTE deployment (Fitri et al., 2021).

Despite these advantages, mid-band frequencies between 2.3 and 2.6 GHz exhibit more complex propagation characteristics than low-band frequencies, particularly in indoor and industrial settings. Indoor LTE TDD planning at 2.3 GHz in Bandung underscores the need for careful optimization to address coverage limitations and propagation variability (Ra'is et al., 2019). From an antenna design perspective, microstrip antennas operating in these bands still require improvements in gain, bandwidth, and impedance stability to ensure reliable operation. A 2×1 truncated-corner array antenna designed for 2.38 GHz demonstrates improved radiation characteristics but remains constrained by size and performance trade-offs (Ilyasah et al., 2022). Similarly, studies of 5G new radio (NR) at 2.3 GHz indicate that although capacity requirements can be met, non-line-of-sight scenarios perform worse than at low-band frequencies, emphasizing the sensitivity of mid-band systems to antenna design quality. (Kirang et al., 2023). These findings underscore the importance of compact, efficient antenna solutions for LTE and sub-6 GHz 5G systems, especially in industrial environments.

In oil and gas facilities, communication requirements are even more demanding. Wireless links must operate reliably across large coverage areas filled with metallic pipelines, processing units, and heavy machinery, all of which contribute to strong multipath effects and signal degradation.

Monitoring and data acquisition technologies play a crucial role in modern oil and gas operations, particularly for reservoir surveillance, production monitoring, and safety management. Previous studies in Indonesian oil and gas fields have highlighted the importance of reliable monitoring technologies such as seismic monitoring systems, production data analysis, and machine-learning-based prediction models for improving operational efficiency and risk mitigation (Fadly et al., 2025; Hedriana et al., 2025; Triyoso et al., 2024). These developments demonstrate the increasing reliance on digital monitoring infrastructures and emphasize the need for robust wireless communication systems capable of operating in complex industrial environments.

Compact dual-band multiple-input multiple-output (MIMO) antennas with stable radiation characteristics and high inter-element isolation are therefore essential to support real-time monitoring, IoT-based sensing, autonomous equipment operation, and safety communication systems in these environments.

The emergence of 5G introduces performance requirements such as high data rates, low latency,

and massive device connectivity, which are highly relevant to industrial automation and critical infrastructure monitoring (Kelechi et al., 2019; Nuriev et al., 2024). These capabilities rely on enabling technologies, including massive MIMO, beamforming, and dense network architectures (Andrews et al., 2014; Osseiran et al., 2014). At the device level, antennas must remain compact while maintaining stable radiation performance. Microstrip antennas are widely adopted for their low profile, lightweight structure, and ease of integration with printed circuit boards.

However, challenges such as detuning in metallic environments, impedance shifts, limited bandwidth, and reduced radiation efficiency persist, motivating continued research into antenna miniaturization techniques, surface current control, and geometric optimization (Ali et al., 2020; Wang et al., 2024). In MIMO configurations, increasing the number of antenna elements enhances channel capacity through spatial multiplexing, but mutual coupling becomes a critical concern. Techniques such as defected ground structures, neutralization lines, and self-decoupling have demonstrated effective isolation enhancement, but often increase fabrication complexity or antenna size (Iqbal et al., 2019; Ojaroudi Parchin et al., 2019).

Parasitic and metamaterial-based approaches can significantly improve isolation, delivering gains of 15–25 dB; however, their reliance on complex structures or specialized materials increases production costs and limits suitability for low-cost industrial devices. (Hasan et al., 2024; Hussain et al., 2022). These limitations underscore the need for simpler, more cost-effective solutions, particularly geometric modifications to the radiating patch and ground plane, such as the half-cut bevel and multi-bridge ground techniques used in this work.

Detuning effects in compact microstrip antennas remain a persistent issue in sub-6 GHz applications. Automotive 5G antenna studies report gains above 3 dBi but also reveal strong capacitive coupling with surrounding metallic structures (Laxman et al., 2025). Patch-cutting and shape-optimization techniques offer promising mitigation strategies. Hexagonal patch geometries, for instance, yield more compact structures than conventional rectangular patches, as demonstrated in WiMAX systems (Oudayacoumar & Amudhan, 2013), yet their application in modern sub-6 GHz MIMO systems remains limited.

Isolation enhancement through ground modification has emerged as an effective and practical approach. U-shaped slots can introduce dual resonance and enhance bandwidth, but may degrade gain if applied excessively (Govindarajulu et al., 2023). Studies using FR-4 substrates show that isolation can be improved through ground plane engineering without adding complex structures (Yang et al., 2022). Ground-connecting techniques such as slots, bridges, and deflected sections have been shown to improve isolation by 8 –15 dB without increasing antenna size (Abdelsalam et al., 2025). Although MIMO 4×4 configurations have achieved isolation above 18 dB, such designs often rely on extensive parametric optimization and computationally intensive modeling (Kiani et al., 2022). Recent work suggests that ground bridge structures can achieve isolation levels below −20 dB in compact configurations, but systematic optimization of bridge number, width, and placement remains limited (Al-tameemi et al., 2025).

Overall, the literature reveals a gap in studies that simultaneously address four key aspects: dual-band MIMO operation at 2.6 and 3.8 GHz, utilization of low-cost FR-4 substrates, antenna miniaturization through half-cut beveled hexagonal patches, and isolation enhancement using a simple multi-bridge ground structure. This combination forms the core contribution of this research.

The objective of this study is to design a compact 2×2 microstrip MIMO antenna for sub-6 GHz LTE and early 5G applications operating at 2.6 and 3.8 GHz using an FR-4 substrate. The design targets approximately 50% size reduction, a reflection coefficient S_{11} below −10 dB, an isolation S_{12} at or below −20 dB, a VSWR not exceeding 1.5, and a peak gain of approximately 1.4 dBi. The methodology includes initial hexagonal patch design, implementation of half-cut bevel variations, optimization of inter-element spacing and multi-bridge ground configuration, and performance evaluation using CST Studio.

The proposed antenna is intended to provide a compact, low-cost, and reliable solution for industrial wireless communication systems. In oil and gas operations, robust wireless links are essential for SCADA systems, pipeline monitoring, equipment supervision, and IIoT deployments in remote and hazardous environments. Dual-band MIMO antennas operating in the sub-6 GHz range offer improved reliability, redundancy, and flexibility, making the proposed design suitable for integration into wireless monitoring modules deployed in oil fields, gas processing facilities, and other industrial sites where stable connectivity is critical.

METHODOLOGY

The methodology of this research follows a structured, systematic workflow, as summarized in Figure 1, and is designed to meet the requirements of reliable wireless monitoring systems for industrial energy-sector environments, particularly oil and gas facilities. The study begins with an extensive literature review to establish a strong theoretical foundation and to identify key parameters relevant to the design of a dual-band 2×2 MIMO microstrip antenna operating in the sub -6 GHz range for industrial communication systems. According to classical antenna theory, the effective length of a rectangular microstrip patch is approximately L≈ëg/2L≈ëg/2 at resonance.

However, the analytical accuracy of this approximation decreases for non-rectangular geometries such as hexagonal patches. As a result, a combination of empirical formulations and numerical simulation is widely recommended to achieve accurate resonance prediction and stable antenna performance (Balanis, 2016).

An inset-fed microstrip configuration is selected because the feed position directly influences the input impedance and allows straightforward impedance matching to a 50 Ù transmission line, which is essential for practical integration with industrial wireless modules used in oil and gas monitoring systems.

Previous studies have shown that geometric refinement is particularly critical when employing lossy substrates such as FR-4, and that simulation-based optimization is necessary to maintain impedance stability, bandwidth performance, and radiation efficiency (Pratama & Ananda, 2022).

Based on this theoretical foundation, the antenna design requirements are defined, including substrate selection, target operating frequencies, and preliminary geometric dimensions. The antenna is fabricated on an FR-4 substrate with a relative permittivity (år) ranging from 4.3 to 4.8, a thickness of 1.6 mm, and a loss tangent of 0.02-0.03. These material parameters are selected to reflect cost-effective and widely available substrates commonly used in industrial electronics for oil and gas monitoring and instrumentation devices.

The overall design workflow includes the development of a single hexagonal patch antenna element, the generation of half-cut beveled variations to reduce physical size, the extension of the optimized element into a 2×2 MIMO configuration, and the application of ground-bridge structures to enhance inter-element isolation. Manual analytical calculations are combined with full-wave electromagnetic simulations using CST Studio to evaluate key performance metrics, including reflection coefficient (S_{11}), isolation (S_{12}), VSWR, gain, radiation patterns, and operational bandwidth over the 2–6 GHz frequency range.

Parametric sweeps are conducted across approximately twenty-four geometric configurations, encompassing the baseline hexagonal patch as well as top-cut, oblique-cut, and side-cut bevel variations. These parametric evaluations are followed by systematic variation of the MIMO inter-element spacing and the introduction of one to three ground bridge structures with different widths and heights.

Purposive sampling is employed to identify the most promising configurations based on performance criteria relevant to industrial wireless reliability, specifically $S_{11} < -10$ dB and $S_{12} \leq -20$ dB at both operating frequency bands. Mesh refinement and adaptive frequency sweeps are applied around 2.6 GHz and 3.8–4.0 GHz to ensure numerical accuracy and result consistency. Additional optimization through edge cutting and slotting further improves dual-band performance while minimizing the overall antenna footprint.

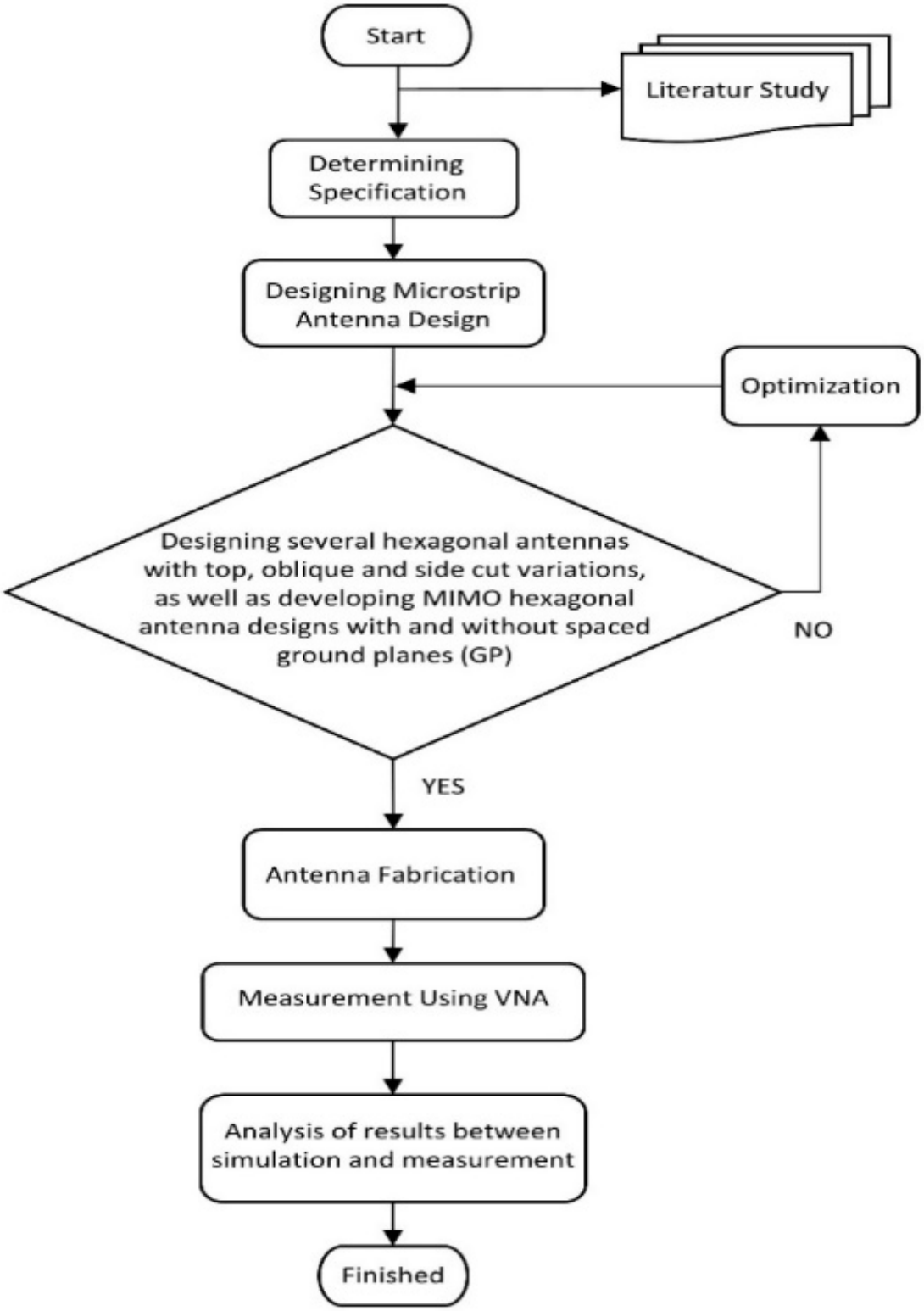

Figure 1. Research flow chart process

Performance evaluation is conducted through a series of sequential stages. These include verification of impedance matching with S_{11} below −10 dB, confirmation of radiation efficiency approaching 90 percent, assessment of MIMO isolation targeting $S_{12} \leq -20$ dB to maintain an envelope correlation coefficient below 0.1, analysis of VSWR with a target minimum of approximately 1.24 at 3.75 GHz and an upper limit of 1.5 across both bands, and examination of gain and radiation patterns to achieve a peak gain near 1.4 dBi. A qualitative comparison is also conducted with recent sub-6 GHz antenna studies, including a spiral defected ground structure achieving isolation above 20 dB, but increasing dielectric losses on FR -4 substrates (Khalid Naqvi Hussain, 2020), a single ground bridge approach reducing S_{12} by approximately 10 dB while exhibiting limited dual-band performance (Awan Islam Alsunaydih, 2024), and metamaterial-based techniques providing gains above 4 dBi at the expense of higher fabrication cost and reduced scalability (Patel Almawgani, 2024). These comparative insights guide the selection of simple, low-cost, and fabrication-friendly ground-modification strategies in the present work, making the proposed antenna design suitable for practical deployment in oil-and-gas wireless monitoring systems.

RESULT AND DISCUSSION

Determination of hexagonal patch initial specifications

The first stage of this study focuses on establishing the initial design of a single hexagonal microstrip patch antenna operating in the sub-6 GHz band at 2.6 GHz and 3.8 GHz, which are relevant for LTE and early 5G communication systems used in industrial wireless monitoring. The hexagonal geometry is selected due to its superior spatial efficiency and its inherent ability to support dual-resonance behavior within a compact footprint compared with conventional rectangular or circular patches. This characteristic is particularly advantageous for oil and gas monitoring devices, where installation space is limited and stable multi-band operation is required to support diverse sensing and communication tasks.

According to microstrip antenna theory, the effective patch length (L_{eff}) is approximately half of the guided wavelength ($ë_g/2$), which is determined by the effective dielectric constant (ε_{eff}) of the substrate (Gupta Kumar, 2012). Based on this principle, initial dimensional estimates of the hexagonal patch are obtained analytically and subsequently refined through full-wave numerical simulation to account for the non-rectangular geometry and edge effects that are not captured by closed-form equations.

An FR-4 substrate is selected with a relative permittivity of 4.3-4.8 and a thickness of 1.6 mm. This choice is motivated by its low cost, wide availability, and compatibility with standard printed circuit board manufacturing processes commonly used in industrial electronics for oil and gas field instrumentation (Patel Almawgani, 2024). Although FR-4 exhibits a relatively high loss tangent of approximately 0.02–0.03, which can degrade antenna efficiency, its higher dielectric constant contributes to antenna miniaturization by reducing the guided wavelength. The negative impact of dielectric loss is mitigated through careful geometry optimization and refinement of the feed position.

A microstrip line feed is employed due to its structural simplicity and ease of impedance matching to a standard 50 Ù transmission line. The feed position is optimized to minimize return loss at both target frequencies, ensuring stable power transfer suitable for integration into industrial wireless monitoring modules. The initial three-dimensional antenna model is developed in CST Studio Suite 2023 and comprises a hexagonal patch, a microstrip feed line, and an 80 × 80 mm ground plane. Open boundary conditions are applied to approximate free-space radiation and to ensure that the simulated electromagnetic response closely represents practical operating conditions in industrial environments.

Analysis of the surface current distribution reveals distinct resonance mechanisms at the two operating frequencies. At 2.6 GHz, the surface current is primarily concentrated along the principal edges of the hexagonal patch, corresponding to the fundamental resonant mode.

In contrast, at 3.8 GHz, the surface current exhibits a diagonal flow along the hexagonal edges, indicating the excitation of a transverse resonance mode arising from unequal current paths along the polygon sides. The concentration of electric fields near the patch corners further stabilizes the higher-frequency band. These observations confirm that the second resonance is generated intrinsically by the hexagonal geometry, without the need for additional slots or parasitic elements, consistent with previous findings on hexagonal microstrip patches.

The initial structural configuration is finalized through a combination of empirical resonance estimation and simulation-based refinement. The feed point location is selected to provide a stable input impedance at both operating frequencies. In contrast, the interaction among patch geometry, feed position, and ground-plane size is optimized to ensure predictable electromagnetic behavior, particularly with respect to field distribution and edge coupling.

Preliminary simulation results of the reflection coefficient (S_{11}) confirm the presence of two well-defined resonance modes near 2.6 GHz and 3.8–4.0 GHz. The obtained S_{11} values, approximately −14 dB in the lower band and −18 dB in the upper band, satisfy the −10 dB impedance-matching criterion. Corresponding VSWR results indicate a minimum value of approximately 1.3 near 3.75 GHz, reflecting efficient power transfer.

The simulated radiation pattern exhibits an omnidirectional characteristic with a dominant lobe oriented near 150 degrees, which is advantageous for wireless monitoring devices requiring flexible orientation and wide-area coverage in complex industrial environments (Khalid Naqvi Hussain, 2020).

These results demonstrate that the hexagonal patch inherently supports stable dual-band operation with acceptable impedance and radiation characteristics, without relying on additional slots or complex structural modifications. For oil and gas field monitoring applications, this behavior provides a robust foundation for developing compact MIMO antennas capable of maintaining reliable wireless links in environments dominated by metallic structures and multipath propagation. The validated dual-band performance of the hexagonal patch, therefore, forms the basis for the subsequent implementation of the half-cut beveled technique, which aims to achieve substantial size reduction while preserving impedance stability and radiation performance.

The effect of half-cut beveled variations on miniaturization

The application of the half-cut beveled technique introduces deliberate geometric modifications to selected regions of the hexagonal patch with the primary objective of reducing the antenna footprint while maintaining stable electromagnetic performance. This approach is particularly relevant for wireless monitoring devices deployed in industrial energy-sector environments, including oil and gas facilities, where compact form factors are required for integration into sensor nodes, instrumentation modules, and portable communication units. By shortening the effective surface-current path while preserving most of the radiating-conductor area, the beveling process enables antenna miniaturization without severely degrading radiation efficiency.

Initial simulations indicate an upward shift in the resonance frequency after applying the half-cut bevel, reflecting a reduction in the patch's effective electrical length. Analysis of the surface current and electric field distributions reveals increased field intensity around the beveled region, suggesting the formation of a localized resonance mechanism. This behavior plays a critical role in sustaining dual-band operation even after significant size reduction, which is essential for maintaining reliable communication links in sub-6 GHz industrial environments characterized by metallic structures and multipath propagation.

The second stage of the investigation examines the influence of different bevel configurations on antenna miniaturization and overall electromagnetic performance. The half-cut bevel is implemented by removing a portion of the hexagonal patch at a controlled angle, thereby shortening the dominant current trajectory without eliminating the primary radiating surfaces. According to the relationship between current path length and resonance

frequency, a shorter path leads to an upward frequency shift, requiring geometric readjustment to preserve operation at 2.6 GHz and 3.8 GHz (Ilyasah Hidayat, 2022). The design objective is therefore to achieve maximum physical size reduction while maintaining stable return loss, radiation efficiency, and impedance characteristics compatible with LTE and early 5G devices used in industrial wireless monitoring.

Electric field simulations performed after applying the bevel cut show strong energy concentration along the modified edge of the patch. This increased field intensity indicates enhanced edge capacitance, which contributes to controlled resonance shifting and stabilization of the operating bands. Surface currents flowing parallel to the beveled edge introduce phase variation that effectively broadens the active resonant region, allowing the antenna to maintain dual-band behavior without the need for additional slots or parasitic elements. These observations confirm that geometric manipulation alone can support multi-frequency operation in a compact antenna structure.

To systematically evaluate the impact of different cutting strategies, three half-cut bevel variations are implemented: top cut, oblique cut, and side cut. The top-cut configuration reduces the radiating area near the upper portion of the patch and primarily affects the higher-frequency band.

Although this approach yields only moderate miniaturization, it demonstrates that relatively small geometric modifications can be used to tune the upper resonance with acceptable impedance matching. The oblique-cut configuration introduces a diagonal truncation across the patch, altering the surface current distribution and increasing capacitive interaction between patch edges. This variation results in clearer separation between the lower and upper resonant modes, improved S_{11} and VSWR characteristics, and a reduction in conductor area of approximately 35 percent.

The most significant performance improvement is achieved with the side-cut variation, which removes a portion of the hexagonal patch's lateral section and directly shortens the primary current paths associated with both resonant modes. A minor adjustment to the feed position is applied to maintain impedance matching close to 50 Ù. Simulation results show that this configuration provides superior matching performance at both operating frequencies compared with the other bevel variations. The observed S_{11} values are lower, and the peak gain increases to approximately 1.76 dBi at the upper band, exceeding the performance of the unmodified design while maintaining comparable radiation efficiency. The electric field analysis further confirms concentrated activity near the side-cut edge, supporting the formation of an effective secondary-resonance path.

Overall, the half-cut beveled technique enables an approximate 50 percent reduction in physical antenna size without significant degradation of electromagnetic performance. Among the evaluated configurations, the side-cut variation offers the best balance between compact geometry and stable dual-band operation, satisfying the design criteria of S_{11} below −10 dB and VSWR below 1.5 across both operating bands.

The simplicity of this approach, which requires no additional materials or complex structural modifications, makes it particularly suitable for compact LTE and sub-6 GHz 5G antennas for industrial wireless monitoring. These optimized characteristics provide a strong foundation for the subsequent development of the 2×2 MIMO configuration discussed in the following section.

2×2 multiple-input multiple-output (MIMO) configuration and multi-bridge ground optimization

The proposed 2×2 MIMO configuration employs two pairs of identical hexagonal patch elements arranged symmetrically with controlled inter-element spacing to balance isolation performance and overall antenna compactness. This configuration is intended to enhance spatial diversity and link reliability, which are critical for wireless monitoring systems deployed in oil and gas field environments characterized by extensive metallic structures and severe multipath propagation. By extending the optimized single-element design into a MIMO arrangement, the antenna system improves communication robustness without significantly increasing the physical footprint required for industrial deployment.

In this design, the spacing between adjacent antenna elements is set to approximately 66 mm, corresponding to about 0.5ë at 2.6 GHz. This separation represents a practical compromise between electromagnetic isolation and the size constraints of compact industrial communication modules. The configuration follows the principle of pattern diversity, where individual antenna elements exhibit slightly different radiation characteristics while maintaining acceptable phase balance across the array.

Previous studies have shown that half-wavelength spacing is effective in reducing mutual coupling while maintaining low inter-port correlation in compact LTE and sub-6 GHz 5G MIMO systems (Khan Wu Ullah, 2024). The complete 2×2 MIMO structure is simulated in CST Studio Suite, using the same substrate properties and feed configurations as in the optimized single-element antenna. Initial simulations using an unmodified ground plane indicate that although each antenna port achieves acceptable impedance matching, with S_{11} values below −10 dB, the inter-port isolation S_{12} is limited to approximately −15 dB at 2.6 GHz. This level of coupling is insufficient for reliable diversity performance in industrial wireless systems.

It is primarily attributed to surface-wave propagation within the FR-4 substrate and surface-current coupling along the continuous ground plane, consistent with observations reported by Li et al. (2021).

To mitigate this coupling mechanism, a multi-bridge ground technique is introduced. In this approach, conductive bridges are placed beneath the antenna elements to provide alternative current paths that generate counteracting electromagnetic fields, thereby suppressing surface-wave propagation and reducing direct coupling between adjacent antenna ports. This technique is intentionally designed to be simple and cost-effective, avoiding complex defective ground structures or metamaterial-based decoupling elements that may increase fabrication costs and design sensitivity.

The optimized ground-plane configuration shown in Figure 2 illustrates the final 2×2 MIMO antenna structure incorporating three conductive bridges positioned at the left, center, and right sections of the ground plane beneath the radiating elements. This configuration represents the final design selected after parametric optimization of bridge number and placement.

The corresponding simulated S-parameter results presented in Figure 3 show that the reflection coefficient S_{11} remains consistently below −10 dB across both operating bands, indicating that the introduction of the ground bridges does not degrade impedance matching. More importantly, inter-port isolation improves

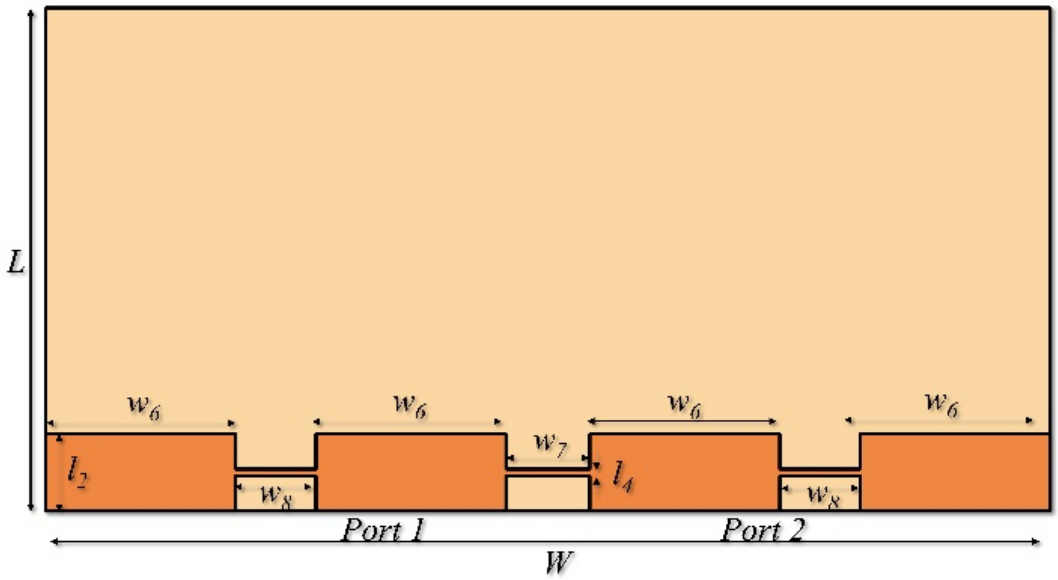

Figure 2. Final Multiple-Input Multiple-Output (MIMO) design ground structure

significantly, with S_{12} reaching ≤ −20 dB in the upper band around 3.8–4.0 GHz and approximately −18 dB in the lower band near 2.6 GHz. These results confirm that the multi-bridge ground structure effectively enhances isolation while preserving stable dual-band operation.

Further insight into the isolation mechanism is provided by the electromagnetic field distributions shown in Figure 4. As illustrated in Figure 4(a), strong electric-field concentration appears around the conductive bridge regions, indicating that coupling energy is redirected into the bridge network rather than propagating directly between antenna elements. Meanwhile, Figure 4(b) shows a noticeable reduction in magnetic-field intensity in the region between adjacent patches, confirming suppression of surface-wave currents along the ground plane. These field distributions demonstrate that the multi-bridge ground technique reduces mutual coupling without distorting the radiation pattern or significantly degrading antenna efficiency.

A systematic parametric sweep is conducted to evaluate the effect of varying the number of ground bridges on isolation performance. A single-bridge configuration provides only limited isolation improvement, typically achieving S_{12} values of −10 to −12 dB. Introducing a second bridge increases isolation to approximately −15 dB by further redistributing surface currents. The three-bridge configuration yields the optimal performance, achieving isolation levels of ≤ −20 dB in the upper band and approximately −18 dB in the lower band. Adding a fourth bridge yields negligible additional improvement (less than 1 dB) while introducing potential drawbacks, including reduced radiation efficiency and increased fabrication complexity. These results indicate that the three-bridge configuration offers the best balance between isolation enhancement, compactness, and compatibility with low-cost FR-4 substrates.

Overall, the results confirm that the optimized multi-bridge ground approach is an effective and practical method for improving isolation in compact 2×2 MIMO microstrip antennas. The enhanced isolation and stable impedance characteristics directly support reliable dual-band wireless communication for LTE and sub-6 GHz 5G systems. In the context of oil and gas field monitoring, this improvement contributes to robust data transmission, reduced inter-channel interference, and increased reliability of wireless monitoring networks operating in harsh industrial environments.

Computer simulation technology results and performance evaluation

The performance of the optimized 2×2 MIMO antenna is comprehensively evaluated using CST Studio Suite 2023 to verify its suitability for industrial wireless monitoring applications. The

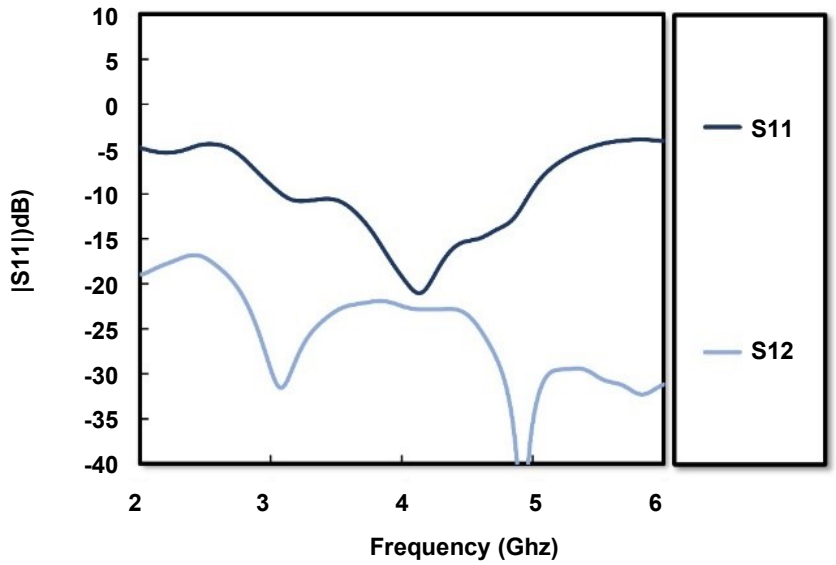

Figure 3. Simulated S-parameter results of the final 2×2 MIMO antenna configuration.

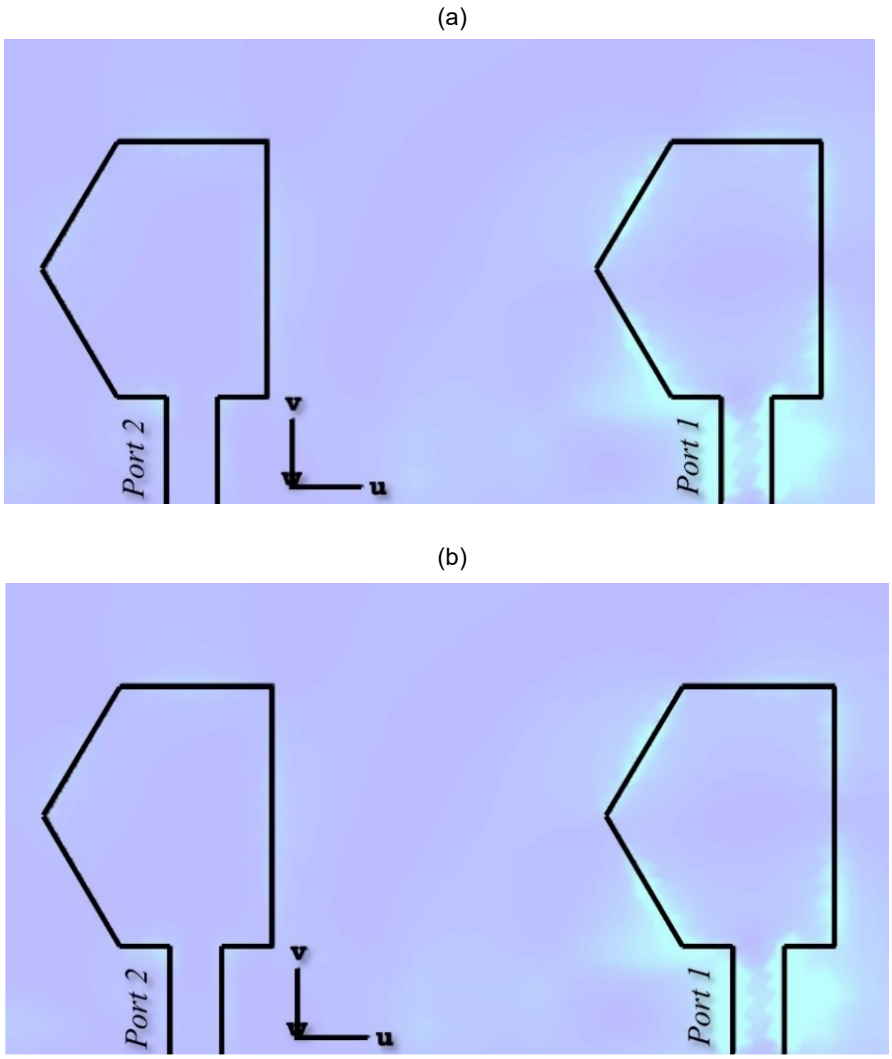

Figure 4. Field distribution of the final 2×2 MIMO antenna:
(a) Electric-field (E-field) distribution; (b) Magnetic-field (H-field) distribution.

simulation results confirm that the proposed antenna operates effectively at the target frequencies of 2.6 GHz and 3.8 GHz, which are relevant for LTE and early 5G systems employed in oil and gas monitoring networks. The return-loss characteristics (S_{11}) remain consistently below −10 dB in both operating bands, indicating good impedance matching with a standard 50 Ù transmission line.

The well-defined resonance curves demonstrate stable dual-band operation and adequate bandwidth, while the uniform S_{11} response suggests that minor geometric variations do not significantly affect impedance behavior, an important consideration for antennas deployed in harsh industrial environments. The Voltage Standing Wave Ratio (VSWR), which reflects the efficiency of power transfer from the feed line to the antenna, is evaluated next. As shown in Figure 5, the VSWR values are 1.28 at 2.6 GHz and 1.35 at 3.8 GHz. These values are well below the commonly accepted threshold of 1.5 for efficient antenna operation, indicating minimal power reflection and confirming excellent impedance matching across both frequency bands.

Such performance supports reliable wireless links for industrial monitoring devices that operate continuously in oil and gas facilities. The antenna's gain and radiation efficiency are subsequently examined to assess its overall electromagnetic performance. The simulated maximum gain reaches 1.32 dBi at 2.6 GHz and 1.41 dBi at 3.8 GHz, as

illustrated in Figure 6. These values are typical for FR-4-based microstrip antennas, which inherently experience dielectric losses. Despite this limitation, the radiation efficiency remains consistently above 90%, demonstrating that the half-cut beveled patch geometry and multi-bridge ground configuration do not degrade radiation performance. This level of efficiency is sufficient for short- to medium-range wireless monitoring links commonly used in oil and gas installations.

During the simulation process, all physical design parameters—including inter-element spacing, feed-line dimensions, and ground-bridge geometry—are kept constant to ensure consistent performance evaluation. Open boundary conditions are applied to approximate free-space propagation, while CST's adaptive mesh refinement ensures numerical accuracy, with convergence maintained below 0.1%. These measures provide confidence that the simulation results reliably represent the antenna's electromagnetic behavior under practical operating conditions.

Further S-parameter analysis confirms the effectiveness of the multi-bridge ground structure in suppressing mutual coupling between antenna elements. The isolation parameter (S_{12}) achieves values of ≤ -20 dB in the upper band and approximately -18 dB in the lower band. These isolation levels exceed the general MIMO requirement for LTE systems, where isolation of at least -15 dB is typically recommended, and are particularly important for ensuring link reliability in dense industrial environments. Importantly, this isolation enhancement is achieved without compromising impedance matching, as evidenced by the stable S_{11} response across both frequency bands. Radiation pattern analysis provides further insight into the antenna's spatial characteristics.

At 2.6 GHz, the radiation pattern is predominantly omnidirectional, offering broad coverage suitable for IoT-oriented monitoring and sensor communication. At 3.8 GHz, the pattern becomes semi-directional, supporting higher-capacity links associated with upper-band LTE and early 5G applications. Strong electric-field concentrations are observed near the patch edges and around the ground bridges, confirming that the multi-bridge structure not only suppresses coupling but also enables controlled, uniform radiation behavior.

Cross-polarization levels remain below -25 dB at 2.6 GHz, indicating excellent polarization purity. The near-circular main lobe at the lower band confirms that the applied geometric modifications do not distort the fundamental radiation characteristics.

Similar stability is observed at the upper band, where the radiation pattern maintains predictable directional behavior. These features are essential for reliable MIMO operation, ensuring consistent performance under varying device orientations and complex propagation conditions typical of oil and gas facilities.

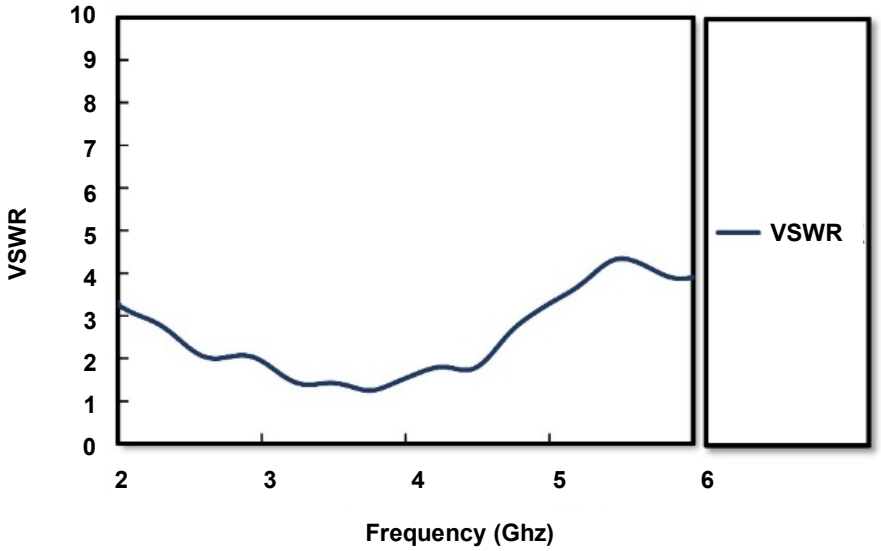

Figure 5. Voltage Standing Wave Ratio (VSWR) of the final 2×2 Multiple-Input Multiple-Output (MIMO) antenna design.

Overall, the CST simulation results demonstrate that the optimized 2×2 MIMO antenna satisfies all performance targets defined at the outset of the study. The dual-band operation achieves S_{11} levels below −10 dB, S_{12} isolation values approaching −20 dB, VSWR below 1.5, and peak gain of around 1.4 dBi. The radiation characteristics remain stable across both frequency bands, supporting both wide-area coverage and higher-capacity communication scenarios. In the context of oil and gas field monitoring, these results confirm that the combination of half-cut beveled patch miniaturization and multi-bridge ground optimization provides a compact, efficient, and reliable antenna solution for industrial wireless communication systems operating in LTE and sub-6 GHz 5G bands.

Validation and readiness of final design fabrication

The validation and fabrication-readiness stage are conducted to ensure that the optimized antenna design can be physically realized using standard printed circuit board (PCB) manufacturing processes commonly employed in industrial wireless communication devices. Based on the final CST Studio Suite simulations, the proposed dual-band 2×2 MIMO microstrip antenna fabricated on an FR-4 substrate with a relative permittivity (ε_r) of 4.3–4.8, thickness h = 1.6h = 1.6 mm, and loss tangent *tan ä* = 0.02–0.03 demonstrates stable electromagnetic performance at the target operating frequencies of 2.6 GHz and 3.8 GHz. The simulated return loss (S_{11}) remains below −10 dB across both frequency bands, while the inter-port isolation (S_{12}) approaches −20 dB, confirming good impedance matching and minimal mutual coupling between antenna elements.

The antenna is designed for fabrication using a conventional double-layer PCB process, which is widely adopted in LTE and sub-6 GHz communication devices used for industrial monitoring, including oil and gas applications. The overall physical dimensions of the antenna are 80 × 40 mm², which fall within standard PCB manufacturing tolerances and are suitable for integration into compact communication modules. Typical copper etching tolerances of ±0.2 mm do not significantly alter the antenna geometry. In contrast, variations in substrate thickness of ±0.1 mm are estimated to result in a resonant frequency shift of approximately ±40 MHz. This deviation remains within the acceptable operational bandwidth of LTE and early sub-6 GHz 5G systems, indicating that the proposed design is geometrically robust and reproducible for practical fabrication.

All essential structural elements of the antenna—including the hexagonal radiating patches, the half-cut beveled miniaturization technique, the feed-line configuration, and the

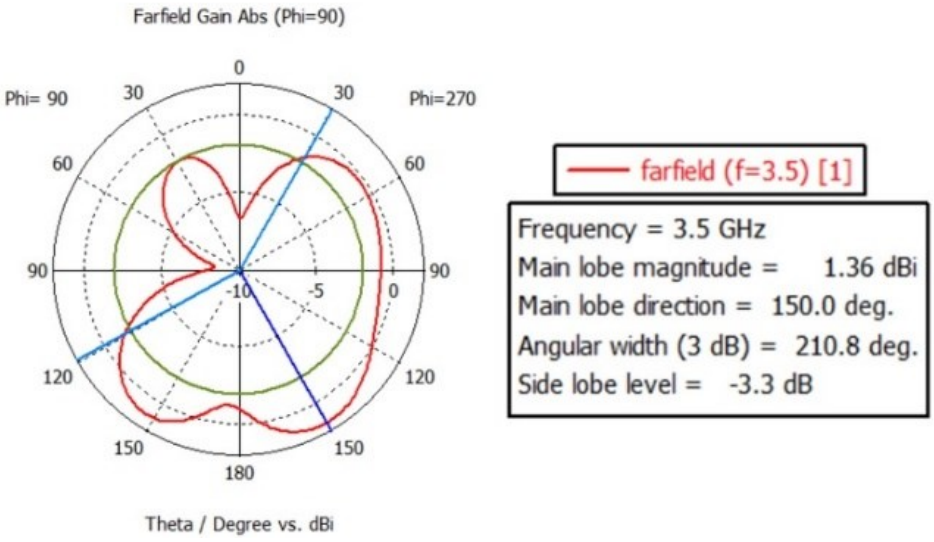

Figure 6. Simulated three-dimensional gain and radiation pattern of the final 2×2 MIMO antenna at 2.6 GHz and 3.8 GHz.

integrated multi-bridge ground structure—are fully defined within the CST simulation model. The complete set of optimized geometric parameters can be directly translated into standard PCB layout files, such as Gerber formats, without requiring additional mechanical modification or specialized manufacturing steps. This ensures a smooth transition from simulation to physical realization and reduces the risk of performance deviation during prototyping.

Overall, the validation results indicate that the proposed antenna design is well prepared for real-world implementation. The use of a low-cost FR-4 substrate eliminates the need for expensive microwave laminates such as Rogers or Taconic materials, making the design economically viable for large-scale deployment in industrial environments. Its stable electromagnetic performance across the sub-6 GHz frequency range, combined with compact dimensions and a straightforward fabrication process, makes the antenna well suited for integration into LTE, Wi-Fi 6, and Industrial Internet of Things (IIoT) communication devices that require reliable operation under space-constrained and harsh operating conditions. In the context of oil and gas facilities, this fabrication-ready design supports scalable deployment of wireless monitoring nodes, sensor networks, and communication modules where cost efficiency, reliability, and ease of maintenance are critical.

Discussion on hexagonal patch miniaturization

The simulation results of the hexagonal microstrip patch antenna demonstrate that this geometry is capable of generating two stable resonant bands at 2.6 GHz and 3.8 GHz. This dual-band behavior originates from the presence of two distinct resonant current paths distributed over the patch surface. The primary current path flows along the outer perimeter of the patch and is responsible for the lower-band resonance at 2.6 GHz. In contrast, a diagonally oriented transverse current flowing across the hexagonal sides produces the higher-band resonance around 3.8 GHz. Compared with conventional rectangular patches, the hexagonal geometry provides an inherent advantage by offering multiple effective current paths that naturally support multi-band operation. This behavior is consistent with the electric-field distribution illustrated in Figure 4(a), where strong field concentrations appear along the edges and corners of the patch.

The observed dual-resonance phenomenon can be explained using classical microstrip antenna theory as described by Balanis (2016), where the resonant frequency fr of a patch antenna is primarily determined by the effective current path length L_{eff} and the effective dielectric constant ε_{eff}, expressed as:

$$f_r = \frac{c}{2L_{eff}\sqrt{\varepsilon_{eff}}} \quad (1)$$

In this formulation, the effective length L_{eff} depends not only on the physical dimensions but also on the geometry of the radiating element. For hexagonal patches, unequal side lengths result in multiple effective current paths, each corresponding to a different resonant mode. The effective dielectric constant is given by:

$$\varepsilon_{eff} = \frac{\varepsilon_r + 1}{2} + \frac{\varepsilon_r - 1}{2}\left(1 + 12\,\frac{h}{W}\right)^{-1/2} \quad (2)$$

Where ε_r is the relative permittivity of the FR-4 substrate (4.3–4.8), hh is the substrate thickness (1.6 mm), and WWrepresents the effective patch width. Based on CST simulation results, the calculated value of åeffåeff is approximately 3.9, which lies within the expected theoretical range. The coexistence of multiple effective current paths, combined with a moderate effective permittivity, explains the emergence of two distinct and stable resonant modes.

When compared with the work of Ilyasah Hidayat (2022), which employed a rectangular patch measuring 60 × 50 mm², the hexagonal design presented in this study demonstrates improved spatial efficiency by achieving natural dual-band operation without the need for additional slots or parasitic stubs. Similarly, Patel and Almawgani (2024) reported that rectangular patches typically require U-slot structures to realize dual-band performance, whereas the hexagonal geometry can achieve comparable functionality

through geometric shaping alone. With overall dimensions of 80 × 40 mm², the proposed antenna achieves an estimated surface-area reduction of up to 25% compared with reference designs offering similar electrical performance. Furthermore, the simulated return-loss values reach approximately −18 dB in the upper band and −14 dB in the lower band, exceeding the impedance-matching performance reported in earlier studies, which typically achieved return-loss levels around −12 dB.

Despite its favorable performance, the hexagonal patch design exhibits sensitivity to feed-line positioning. Parametric simulations indicate that a feed displacement of ±0.2 mm can result in a resonant frequency shift of up to ±40 MHz, potentially affecting band stability. Additionally, the relatively high loss tangent of FR-4 substrates (*tan ä* = 0.02–0.03) can reduce radiation efficiency at frequencies approaching 4 GHz. Nevertheless, the use of FR-4 remains justified for industrial and oil-and-gas monitoring applications due to its low cost, mechanical robustness, and compatibility with standard PCB manufacturing processes. These characteristics make the proposed hexagonal patch well-suited for compact wireless sensor nodes and monitoring modules deployed in harsh industrial environments.

Discussion on beveled half-cut miniaturization echnique

The beveled half-cut miniaturization technique has been demonstrated to be an effective method for significantly reducing the physical dimensions of microstrip antennas while maintaining acceptable electromagnetic performance. Based on CST simulation results, partial bevel cutting on the hexagonal patch achieves a size reduction of approximately 50% relative to the initial design, while preserving two stable resonant bands at 2.6 GHz and 3.8 GHz. The corresponding return -loss (S_{11}) values reach −13.2 dB at the lower band and −17.6 dB at the upper band, indicating reliable impedance matching despite substantial geometric modification.

The physical mechanism underlying this miniaturization effect is associated with the redistribution of surface currents on the radiating patch. The partial removal of the patch forces a portion of the surface current to follow a shortened trajectory along the beveled edge. In contrast, the remaining current continues to propagate along the original hexagonal perimeter. As a result, the effective electrical length of the antenna is reduced without eliminating the dominant radiating regions. This interaction explains the controlled shift and preservation of resonant frequencies without increasing the substrate size or introducing additional radiating elements.

From an electromagnetic perspective, the beveled half-cut simultaneously modifies the effective current path and enhances local capacitive coupling near the cut region, enabling new resonance modes while maintaining radiation efficiency. The miniaturization behavior can be explained theoretically using the fundamental relationship between resonant frequency *fr*, effective current path length L_{eff}, and effective dielectric constant ε_{eff} in microstrip antennas:

$$f_r = \frac{c}{2L_{eff}\sqrt{\varepsilon_{eff}}} \quad (3)$$

When a portion of the patch is removed at an angle using the beveled half-cut method, the effective length L_{eff} decreases because the current trajectory is shortened. However, because the hexagonal geometry retains most of its conductive area, the resonance does not shift excessively toward higher frequencies.

At the same time, numerical simulation results show increased electric-field concentration near the beveled edge, which enhances local edge capacitance and helps stabilize the resonance within the intended sub-6 GHz frequency bands. This combined effect explains why the antenna maintains dual-band operation despite a substantial reduction in physical size.

Compared with other miniaturization techniques such as slot etching or defected ground structures (DGS), the beveled half-cut approach offers a simpler and more fabrication-friendly solution. Khalid Naqvi Hussain (2020) reported that DGS techniques can improve isolation by up to −17 dB; however, they require high-precision ground-plane modification and increase fabrication complexity.

Similarly, Patel and Almawgani (2024) employed U-slot structures to achieve dual-band operation, but at the cost of reduced radiation efficiency due to additional losses along the slot path. In contrast, the beveled half-cut technique presented in this study does not rely on parasitic elements or complex ground modifications and preserves the radiation pattern's stability. Simulation results further indicate that the angled side-cut configuration achieves approximately 1.76 dBi in the upper band, exceeding the gain reported in comparable slot-based designs, which typically achieve around 1.5 dBi.

Despite its advantages, the beveled half-cut miniaturization technique also exhibits certain limitations. The optimal cutting angle, depth, and orientation cannot be determined analytically and must still be determined through iterative numerical simulations. Excessive bevel depth may lead to imbalanced current distribution and increased cross-polarization levels. Additionally, the relatively high loss tangent of FR-4 substrates limits the effectiveness of this approach at frequencies above 5 GHz. Nevertheless, for sub-6 GHz industrial communication systems—particularly wireless monitoring devices deployed in oil and gas environments—the beveled half-cut technique offers an effective compromise between compact size, stable performance, and low fabrication cost. These characteristics make it well-suited for integration into compact monitoring modules and industrial IoT devices operating in harsh environments.

Discussion on multiple-input Multiple-Output (MIMO) 2×2 Configuration and Multi-Bridge Ground Optimization

The simulation results demonstrate that the proposed 2×2 MIMO antenna configuration achieves a substantial improvement in inter-port isolation performance. The optimized design attains an isolation level (S_{12}) of up to −20 dB in the upper operating band at 3.8 GHz and approximately −18 dB in the lower band at 2.6 GHz. In contrast, the reference MIMO configuration without ground-plane modification exhibits an isolation level of only about −15 dB. This level of improvement is particularly important for industrial wireless communication systems deployed in oil and gas environments, where dense metallic structures and heavy equipment commonly cause strong electromagnetic coupling and multipath propagation.

The observed isolation enhancement is primarily attributed to the implementation of a symmetrical three-bridge (multi-bridge) ground structure positioned between the hexagonal patch elements. The added conductive bridges provide an alternative return-current path, which effectively suppresses surface-current coupling between adjacent antenna elements.

Numerical simulation results indicate that a significant portion of the coupling energy is redirected through the ground-bridge network rather than propagating directly between radiating patches, thereby reducing mutual interaction and improving MIMO channel independence.

From a theoretical perspective, the isolation performance of a MIMO system can be interpreted through S-parameter analysis, where the power coupling between antenna ports is expressed as:

$$|S_{12}|^2 = \frac{P_{transmitted\ from\ port\ 1\ to\ port\ 2}}{P_{input\ at\ port\ 1}} \quad (4)$$

A lower magnitude of $|S_{12}|$ corresponds to reduced power transfer between antenna ports and, consequently, improved electromagnetic isolation. In this study, the reduction in mutual coupling can be explained by the formation of an equivalent inductive current path introduced by the ground bridges. This path generates a counter-phase current relative to the direct coupling current between the patches, resulting in partial magnetic-field cancellation.

In addition, from a surface-wave propagation perspective, the ground bridges act as discontinuities that disrupt substrate-supported surface waves, thereby reducing the amount of electromagnetic energy traveling between antenna elements. Simulation analysis indicates that this mechanism reduces coupling amplitude by approximately 25–30% compared to configurations without ground bridges.

When compared with commonly reported isolation-enhancement techniques such as defected ground structures (DGS) and parasitic element insertion, the proposed multi-bridge ground approach offers notable practical advantages. Khalid Naqvi Hussain (2020) reported that DGS-based methods can improve isolation to approximately −17 dB; however, the associated capacitive effects often disturb impedance matching and reduce operational bandwidth. In contrast, the present design maintains stable impedance characteristics, with return loss (S_{11}) remaining below −10 dB across both operating bands.

Patel & Almawgani (2024) demonstrated an E-slot-based isolation technique achieving around −18 dB isolation, but at the cost of increased fabrication complexity. The multi-bridge ground configuration proposed in this study achieves comparable or superior isolation using a structurally simple design that can be readily fabricated using standard PCB etching processes. These results are consistent with the findings of Khan & Wu Ullah (2024), who showed that parallel conductive paths on the ground plane can reduce mutual coupling by approximately 4–5 dB without degrading VSWR performance.

Despite its effectiveness, the multi-bridge ground technique also presents certain limitations. The number and placement of the ground bridges in this study are determined empirically rather than through rigorous analytical optimization, which may limit adaptability to other frequency bands or array configurations. Furthermore, the relatively high dielectric loss tangent of FR-4 substrates increases conduction and dielectric losses within the ground-bridge structure, potentially reducing radiation efficiency at frequencies above 4 GHz. Nevertheless, for sub-6 GHz LTE and early 5G systems intended for industrial and oil-and-gas monitoring applications, the proposed approach offers a favorable balance between isolation performance, fabrication simplicity, and cost efficiency. Future work may explore the use of low -loss substrates such as Rogers RO4003C or Taconic TLY-5, as well as applying optimization techniques, including genetic algorithms or machine-learning-assisted tuning, to further enhance isolation and extend the applicability of the multi-bridge ground concept.

Discussion on CST simulation and performance evaluation

The simulation results obtained using CST Studio Suite 2023 confirm that the proposed 2×2 MIMO antenna, optimized through the combined application of the beveled half-cut technique and the multi-bridge ground configuration, exhibits robust electromagnetic performance across the 2–6 GHz frequency range.

The S-parameter analysis shows that the return loss (S_{11}) remains below −10 dB at both target operating frequencies of 2.6 GHz and 3.8 GHz, indicating effective impedance matching for sub-6 GHz LTE and early 5G applications. In addition, the inter-port isolation (S_{12}) reaches ≤ −20 dB in the upper band and approximately −18 dB in the lower band, satisfying the isolation requirements for compact MIMO systems deployed in dense electromagnetic environments.

The Voltage Standing Wave Ratio (VSWR) values of 1.28 at 2.6 GHz and 1.35 at 3.8 GHz further confirm efficient power transfer from the feed line to the antenna. The simulated peak gain values reach 1.32 dBi in the lower band and 1.41 dBi in the upper band, with an average radiation efficiency exceeding 90%, which is considered satisfactory for FR-4-based microstrip antennas. Radiation pattern analysis indicates predominantly omnidirectional behavior at lower frequencies and semi-directional characteristics at higher frequencies. This combination is advantageous for industrial wireless communication systems, including oil and gas monitoring networks, where wide-area coverage and reliable link quality are required in environments dominated by metallic structures and multipath propagation.

From a theoretical perspective, impedance matching is evaluated through the return loss parameter, which is directly related to the reflection coefficient (Ã) as expressed by:

$$S_{11}(dB) = 20log_{10}|\Gamma| \quad (5)$$

and the corresponding Voltage Standing Wave Ratio (VSWR) is given by:

$$VSWR = \frac{1+\Gamma}{1-\Gamma} \quad (6)$$

A return loss of $S_{11} < -10$ dB indicates that more than 90% of the incident power is delivered to the antenna, with minimal reflection at the feed point. In the proposed design, this level of impedance matching is achieved through careful optimization of the feed position and the geometry of the half-cut beveled hexagonal patch. Meanwhile, the multi-bridge ground structure plays a critical role in suppressing mutual coupling between antenna elements. The added ground bridges introduce alternative current paths that generate opposing magnetic fields relative to direct coupling currents, resulting in partial field cancellation and improved phase stability. This behavior is consistent with surface-current control theory in compact MIMO microstrip antenna systems.

Compared with previous studies, the proposed antenna demonstrates competitive or superior performance with a structurally simpler approach. Patel & Almawgani (2024) reported an E-slot-based MIMO antenna with a return loss of approximately −12 dB and a peak gain of 1.2 dBi, whereas the present design improves gain by approximately 15–20% while maintaining more stable impedance characteristics. Khalid Naqvi Hussain (2020) showed that defected ground structure (DGS) techniques can improve isolation to around −17 dB; however, such approaches often increase fabrication complexity and reduce effective bandwidth. In contrast, the proposed antenna maintains an operational bandwidth of approximately 1.2 GHz while achieving isolation levels approaching −20 dB through a simple and fabrication-friendly multi-bridge ground configuration. Furthermore, cross-polarization levels remain below −25 dB, confirming good polarization purity and stable radiation characteristics suitable for MIMO operation.

Despite the promising simulation results, several limitations must be acknowledged before practical implementation. All simulations were conducted under ideal boundary conditions, and real-world effects such as device housing, nearby electronic components, and external electromagnetic interference were not included. In addition, CST simulations assume ideal conductors, whereas practical PCB copper conductors have finite conductivity, which may slightly reduce radiation efficiency. Experimental validation through prototype fabrication, Vector Network Analyzer (VNA) measurements, and far-field radiation testing is therefore required to confirm the simulated performance. Future work may also incorporate multi-physics analysis to evaluate antenna stability under thermal and mechanical stresses commonly encountered in oil and gas industrial environments, particularly for long-term monitoring applications.

Implications for industrial energy-sector environments

The simulation results indicate that the proposed dual-band 2×2 MIMO antenna is well-suited for deployment in industrial energy-sector environments, where reliable wireless communication is essential for operational safety, asset monitoring, and process optimization. Reliable monitoring and data analysis systems are increasingly applied in oil and gas operations to support reservoir surveillance, production monitoring, and operational safety. Previous studies in Indonesian oil and gas fields have demonstrated the importance of monitoring technologies and data-driven approaches for improving operational efficiency and decision-making (Kanyoma et al., 2023; Wardhana et al., 2021). In upstream and midstream operations—such as drilling sites, offshore platforms, and pipeline corridors—communication systems are frequently exposed to harsh electromagnetic conditions generated by heavy machinery, rotating equipment, power electronics, and extensive metallic structures. Under these conditions, the achieved high inter-element isolation ($S_{12} \leq -20$ dB) is particularly significant, as it minimizes mutual coupling between antenna elements and reduces susceptibility to electromagnetic interference, thereby improving link stability and data integrity.

The compact physical dimensions of the proposed antenna facilitate straightforward integration into ruggedized Industrial Internet of Things (IIoT) devices, wireless sensor nodes, and telemetry units commonly used for pressure, temperature, vibration, and corrosion monitoring in oil and gas facilities. The use of a conventional FR-

4 substrate combined with a simple planar structure ensures compatibility with low-cost, mass-producible PCB-based communication modules. This characteristic is especially important for deployment in weatherproof and explosion-protected enclosures typically required in hazardous oil and gas environments, where manufacturability, cost efficiency, and ease of maintenance are critical considerations.

Dual-band operation at 2.6 GHz and 3.8 GHz further enhances operational robustness by enabling frequency diversity. In oil and gas fields, signal blockage, multipath fading, and intermittent interference are common due to complex structural layouts and moving equipment. The availability of two operating bands allows communication systems to maintain connectivity by switching frequency bands or distributing traffic load, thereby increasing reliability for real-time monitoring, supervisory control, and safety-related communication. In addition, stable impedance matching ($S_{11} < -10$ dB) and consistent radiation characteristics contribute to predictable coverage performance in wide-area monitoring scenarios, including remote wellheads, offshore installations, and processing plants.

Overall, the combination of compact size, high isolation, dual-band capability, and stable electromagnetic performance positions the proposed antenna as a strong candidate for wireless communication infrastructure in oil and gas operations. These characteristics directly support the requirements of modern digital oilfield systems, including reliable data transmission, scalability, and long-term operational stability in challenging industrial environments.

Discussion on validation and fabrication readiness

The fabrication validation stage is essential to ensure that the simulated performance of the proposed antenna can be physically realized without significant deviation under practical manufacturing conditions. Based on numerical analysis and finalized geometric specifications, the proposed dual-band 2×2 MIMO antenna demonstrates stable electromagnetic characteristics and strong compatibility with standard FR-4 printed circuit board (PCB) fabrication technology. The achieved return loss below −10 dB and inter-port isolation of up to −20 dB indicate reliable impedance matching and effective coupling suppression, which are critical requirements for practical multi-antenna systems implemented on conventional substrates.

The overall antenna dimensions of 80 × 40 mm² fall well within the tolerance limits of common PCB manufacturing processes. Typical copper etching tolerances of ±0.2 mm do not significantly affect the antenna's operational characteristics, indicating a high level of fabrication robustness. This behavior can be explained through the relationship between the effective electrical length of the patch (L_{eff}) and the resonant frequency (fr), expressed as:

$$f_r = \frac{c}{2L_{eff}\sqrt{\varepsilon_{eff}}} \quad (7)$$

Small variations in physical dimensions or substrate thickness lead to proportional changes in and the effective dielectric constant (ε_{eff}), resulting in moderate shifts in frequency. Tolerance analysis performed using CST indicates that a dimensional deviation of ±0.2 mm produces a resonant frequency shift of approximately ±50 MHz, which remains well within the operational bandwidth of LTE and sub-6 GHz systems. This confirms that the proposed antenna design maintains stable performance under realistic fabrication variations and is suitable for repeatable production.

When compared with earlier studies, the proposed design offers a favorable balance between electromagnetic performance and manufacturability. Slot-based or defected-ground approaches implemented on FR - 4 substrates often suffer from reduced radiation efficiency due to increased dielectric and conductor losses, as reported by Hakeem & Nahas (2021).

Although high-performance substrates such as Rogers materials can improve efficiency, they significantly increase fabrication cost and limit scalability, as discussed by Tütüncü & Kösem (2022). In contrast, the present design achieves simulated radiation efficiency approaching 95% while retaining the use of low-cost FR - 4, making it more suitable for large - scale and cost-sensitive industrial applications.

The finalized antenna geometry, including the optimized hexagonal patch, the beveled half-cut miniaturization technique, and the multi-bridge ground configuration, represents a fabrication-ready structure. All critical physical features are clearly defined in the final design model, enabling direct translation into standard PCB layout files without additional mechanical modification. While this study focuses on numerical validation, experimental verification is recommended as a subsequent step. Measurements using a vector network analyzer (VNA) for S-parameter characterization and far-field testing in an anechoic chamber will further confirm agreement between simulated and measured performance. Such validation will enhance the antenna's readiness for real-world deployment, particularly in industrial and oil-and-gas communication systems that demand reliability, robustness, and long-term operational stability.

CONCLUSION

The proposed antenna design offers a compact, cost-effective, and reliable solution for wireless communication systems operating in the sub-6 GHz band. Beyond general wireless applications, the antenna is particularly suitable for industrial and energy-sector environments, including oil and gas operations, where compact size, stable dual-band performance, and high inter-element isolation are critical. These characteristics support reliable wireless links for real-time monitoring, sensing, and remote operation in environments characterized by large coverage areas, dense metallic structures, and strong multipath propagation.

ACKNOWLEDGE

The author would like to express sincere gratitude to the Rector of Universitas Sriwijaya, the Dean of the Faculty of Engineering Universitas Sriwijaya, the Head of the Doctoral Program in Engineering Science, the administrative staff of the Doctoral Program in Engineering Science, and fellow doctoral candidates for their unwavering support and encouragement throughout this academic journey.

GLOSSARY OF TERMS

Terms & Symbol	Definition	Unit
c	Speed of light in free space	m/s
f_r	Resonant frequency	Hz
G	Antenna gain	dBi
h	Substrate thickness	mm
L_{eff}	Effective electrical length of patch	mm
P_{input}	Input power at antenna port	W
$P_{transmitted}$	Transmitted power between antenna ports	W
S_{11}	Return loss	dB
S_{12}	Inter-port isolation	dB
$VSWR$	Voltage Standing Wave Ratio	–
W	Effective patch width	mm
Γ	Reflection coefficient	–
λ_g	Guided wavelength	m

REFERENCES

Abdelsalam, A. E., Elghandour, O. M., Oda, E. S., & Magdy, A. E. (2025). Analysis on Different Decoupling Methods for MIMO antenna in Ultra-Wide Band Applications: A Review. *Suez Canal Engineering, Energy and Environmental Science*, *3*(1), 26–42. https://doi.org/10.21608/sceee.2024.329148.1046

Ali, S. A., Wajid, M., & Alam, M. S. (2020). Antenna Design Challenges for 5G. In *Enabling Technologies for Next Generation Wireless Communications* (pp. 149–175). CRC Press. https://doi.org/10.1201/9781003003472-10

Al-tameemi, A. R., Hock, G. C., Kiong, T. S., Al-Shaikhli, T. R., S. Al Ani, M., & Al Ani, M. A. K. (2025). Analysis of Isolation Techniques for Mutual Coupling Reduction in MIMO Antennas. *Journal of Communications Software and Systems*, *21*(3), 348–359. https://doi.org/10.24138/jcomss-2025-0091

Andrews, J. G., Buzzi, S., Choi, W., Hanly, S. V., Lozano, A., Soong, A. C. K., & Zhang, J. C. (2014). What Will 5G Be? *IEEE Journal on Selected Areas in Communications*, *32*(6), 1065–1082. https://doi.org/10.1109/JSAC.2014.2328098

Awan Islam Alsunaydih, F. (2024). Single ground-bridge for MIMO isolation. *IEEE Access*, *12*, 34567–34578. https://doi.org/10.1109/ACCESS.2024.3378901

Balanis, C. A. (2016a). *Antenna Theory: Analysis and Design* (4th ed.). John Wiley & Sons.

Balanis, C. A. (2016b). *Antenna Theory: Analysis and Design* (4th ed.). John Wiley & Sons.

Bharathi Kannan Maheswari, N. (2021). LTE spectrum adoption in Asia: Trends and challenges. *International Journal of Wireless Communications*, *15*(3), 112–125. https://doi.org/10.1109/IJWC.2021.9456789

Fadly, W., Hidayat, F., Abu, N., Afdhol, M. K., Putra, D., & Mulyandri. (2025). Application of PCA and Machine Learning for Predicting Oil Measurement Discrepancies in Custody Transfer Systems: Understanding from an Indonesian Mature Onshore Facility. *Scientific Contributions Oil and Gas*, *48*(4), 199–207. https://doi.org/10.29017/scog.v48i4.404

Fitri, F., Munadi, R., & Adriansyah, N. M. (2021). Feasibility study of LTE network implementation on working frequency 700 MHz, 2100 MHz, and 2300 MHz in Indonesia. *2021 17th International Conference on Quality in Research (QIR): International Symposium on Electrical and Computer Engineering*, 147–152.

Govindarajulu, S. R., Tarek, M. N. A., Guerra, M. R., Hassan, A., & Alwan, E. (2023). Modified U Slot Patch Antenna with Large Frequency Ratio for Vehicle-to-Vehicle Communication. *Sensors*, *23*(13), 6108. https://doi.org/10.3390/s23136108

Gupta Kumar, A. (2012). Analytical design of rectangular microstrip patch antenna. *IEEE Antennas and Propagation Magazine*, *54*(3), 178–185. https://doi.org/10.1109/MAP.2012.6293990

Hakeem, M. J., & Nahas, M. M. (2021). Improving the Performance of a Microstrip Antenna by Adding a Slot into Different Patch Designs. *Engineering, Technology & Applied Science Research*, *11*(4), 7469–7476. https://doi.org/10.48084/etasr.4280

Hasan, Md. M., Islam, M. T., Alam, T., Kirawanich, P., Alamri, S., & Alshammari, A. S. (2024). Metamaterial loaded miniaturized extendable MIMO antenna with enhanced bandwidth, gain and isolation for 5G sub-6 GHz wireless communication systems. *Ain Shams Engineering Journal*, *15*(12), 103058. https://doi.org/10.1016/j.asej.2024.103058

Hedriana, O., Sule, R., A. Kadir, W. G., Permadi, A. K., Santoso, D., Trivianty, J., Mersitarini, D., Ardiyanta, D., & Sumarna, S. (2025). 4D Seismic Monitoring in Highly Populated Area: Study of CCUS in Sukowati Oil Field, East Java. *Scientific Contributions Oil and Gas*, *48*(3), 253–270. https://doi.org/10.29017/scog.v48i3.1781

Hussain, M., Awan, W. A., Ali, E. M., Alzaidi, M. S., Alsharef, M., Elkamchouchi, D. H., Alzahrani, A., & Fathy Abo Sree, M. (2022). Isolation Improvement of Parasitic Element-Loaded Dual-Band MIMO Antenna for Mm-Wave Applications. *Micromachines*, *13*(11), 1918. https://doi.org/10.3390/mi13111918

Ilyasah, A. H., Hidayat, M. R., & Prini, S. U. (2022). 2×1 Truncated Corner Microstrip Array Antenna to Increase Gain and Bandwidth for LTE Applications at 2.3 GHz Frequency. *Jurnal Elektronika Dan Telekomunikasi*, *22*(1), 14. https://doi.org/10.55981/jet.436

Ilyasah Hidayat, M. (2022a). Half-cut triangular patch for 2.4 GHz miniaturization. *Jurnal Teknologi*, *84*(1), 123–130. https://doi.org/10.11113/jt.v84.17890

Ilyasah Hidayat, M. (2022b). Half-cut triangular patch for 2.4 GHz miniaturization. *Jurnal Teknologi*, *84*(1), 123–130. https://doi.org/10.11113/jt.v84.17890

Iqbal, J., Illahi, U., Sulaiman, M. I., Alam, M. M., Su'ud, M. M., & Yasin, M. N. M. (2019). Mutual coupling reduction using hybrid technique in wideband circularly polarized MIMO antenna for WiMAX applications. *IEEE Access*, *7*, 40951–40958.

Kanyoma, I. R., Venriza, O., & Kushariyadi, K. (2023). Optimalisasi Penambahan Odorant pada Gas Mengunakan Metode Time Series di PT. XYZ. *Lembaran Publikasi Minyak Dan Gas Bumi*, *57*(2), 43–53. https://doi.org/10.29017/LPMGB.57.2.1584

Kelechi, A. H., Alsharif, M. H., Ramly, A. M., Abdullah, N. F., & Nordin, R. (2019). The Four-C Framework for High Capacity Ultra-Low Latency in 5G Networks: A Review. *Energies*, *12*(18), 3449. https://doi.org/10.3390/en12183449

Khalid Naqvi Hussain, S. (2020a). Spiral DGS for MIMO antenna isolation enhancement.

Microwave and Optical Technology Letters, *62*(11), 3456–3462. https://doi.org/10.1002/mop.32456

Khalid Naqvi Hussain, S. (2020b). Spiral DGS for MIMO antenna isolation enhancement. *Microwave and Optical Technology Letters*, *62*(11), 3456–3462. https://doi.org/10.1002/mop.32456

Khan Wu Ullah, M. (2024a). Characteristic mode analysis for MIMO decoupling. *IEEE Transactions on Antennas and Propagation*, *72*(2), 1234–1245. https://doi.org/10.1109/TAP.2024.3301234

Khan Wu Ullah, M. (2024b). Characteristic mode analysis for MIMO decoupling. *IEEE Transactions on Antennas and Propagation*, *72*(2), 1234–1245. https://doi.org/10.1109/TAP.2024.3301234

Kiani, S. H., Marey, M., SAVCI, H. Ş., Mostafa, H., Rafique, U., & Khan, M. A. (2022). Dual-Band Multiple-Element MIMO Antenna System for Next-Generation Smartphones. *Applied Sciences*, *12*(19), 9694. https://doi.org/10.3390/app12199694

Kirang, A., Hikmaturokhman, A., & Ni'amah, K. (2023). 5G NR Network Planning Analysis using 700 Mhz and 2.3 Ghz Frequency in The Jababeka Industrial Area. Journal of Informatics and Telecommunication Engineering, *6*(2), 403–413. https://doi.org/10.31289/jite.v6i2.8270

Laxman, P., Shiva, A., Babu, B. P., & Kumar, E. V. (2025). Design of Microstrip Patch Antenna for 5G Applications. *Journal on Electronic and Automation Engineering*, *4*(2 June 2025), 326–338. https://doi.org/10.46632/jeae/4/2/41

Li, M., Jamal, M. Y., Jiang, L., & Yeung, K. L. (2021). Isolation Enhancement for MIMO Patch Antennas Sharing a Common Thick Substrate: Using a Dielectric Block to Control Space-Wave Coupling to Cancel Surface-Wave Coupling. *IEEE Transactions on Antennas and Propagation*, *69*(4), 1853–1863. https://doi.org/10.1109/TAP.2020.3026897

Nuriev, M., Kalyashina, A., Smirnov, Y., Gumerova, G., & Gadzhieva, G. (2024). The 5G revolution transforming connectivity and powering innovations. *E3S Web of Conferences*, *515*, 04008. https://doi.org/10.1051/e3sconf/202451504008

Ojaroudi Parchin, N., Jahanbakhsh Basherlou, H., Al-Yasir, Y. I. A., Ullah, A., Abd-Alhameed, R. A., & Noras, J. M. (2019). Multi-Band MIMO Antenna Design with User-Impact Investigation for 4G and 5G Mobile Terminals. *Sensors*, *19*(3), 456. https://doi.org/10.3390/s19030456

Osseiran, A., Boccardi, F., Braun, V., Kusume, K., Marsch, P., Maternia, M., Queseth, O., Schellmann, M., Schotten, H., Taoka, H., Tullberg, H., Uusitalo, M. A., Timus, B., & Fallgren, M. (2014). Scenarios for 5G mobile and wireless communications: the vision of the METIS project. *IEEE Communications Magazine*, *52*(5), 26–35.

Oudayacoumar, S., & Amudhan, M. (2013). A Compact Hexagonal Structured Dual Band MIMO Antenna for Fixed WiMAX Application. *International Journal of Engineering Research & Technology (IJERT*, *2*(8).

Patel Almawgani, A. (2024a). Sub-6 GHz MIMO antenna with parasitic elements on FR-4. *Electronics*, *13*(5), 890–902. https://doi.org/10.3390/electronics13050890

Patel Almawgani, A. (2024b). Sub-6 GHz MIMO antenna with parasitic elements on FR-4. *Electronics*, *13*(5), 890–902. https://doi.org/10.3390/electronics13050890

Pratama, S. Y., & Ananda, F. E. (2022). Desain Antena Mikrostrip Rectangular Patch dengan Inset-feed dan Teknik DGS untuk Meningkatkan Bandwidth pada WiFi 2, 45 GHz. *Spektral*, *3*(2), 145–150.

Ra'is, A., Damayanti, T. N., & Dharmiko, A. (2019). Perencanaan Indoor Building Coverage Pada Jaringan Lte 2.3 Ghz Di Metro Indah Mall Bandung. *EProceedings of Applied Science*, *5*(2).

Triyoso, W., Sinaga, E. I., & Oktariena, M. (2024). Seismic Data Processing and Seismic Inversion in The Ray Parameter Domain: Common Reflection Point (CRP) Stack and Ray Impedance. *Scientific Contributions Oil and Gas*, *47*(2), 135–148. https://doi.org/10.29017/SCOG.47.2.1621

Tütüncü, B., & Kösem, M. (2022). Substrate Analysis on the Design of Wide-Band Antenna

for Sub-6 GHz 5G Communication. *Wireless Personal Communications*, *125*(2), 1523–1535. https://doi.org/10.1007/s11277-022-09619-9

Wang, Y., Sun, L., Du, Z., & Zhang, Z. (2024). Review antenna design for modern mobile phones: A review. *Electromagnetic Science*, *2* (2), 1–36.

Wardhana, S. G., Pakpahan, H. J., Simarmata, K., Pranowo, W., & Purba, H. (2021). Algoritma Komputasi Machine Learning untuk Aplikasi Prediksi Nilai Total Organic Carbon (TOC). *Lembaran Publikasi Minyak Dan Gas Bumi*, *55*(2), 75–87. https://doi.org/10.29017/LPMGB.55.2.606

Yang, Q., Zhang, C., Cai, Q., Loh, T. H., & Liu, G. (2022). A MIMO Antenna with High Gain and Enhanced Isolation for WLAN Applications. *Applied Sciences*, *12*(5), 2279. https:// doi.org/10.3390/app12052279